



A Novel Self-Adaptive Rectifier with High Efficiency and Wide Input Power Range

Shimiao Lai, Zihao Zhang, Zhijun Liu, Ge Wang, Yongjie Zhou, Huacheng Zhu  and Yang Yang * 

College of Electronics and Information Engineering, Sichuan University, Chengdu 610065, China

* Correspondence: yyang@scu.edu.cn

Abstract: A novel 2.45 GHz self-adaptive rectifier with high efficiency and a wide input power range is proposed in this paper. It consists of a high-power sub-rectifier branch, a low-power sub-rectifier branch, an impedance transform and isolation network (ITIN), and a feedback network. Impedance matching is realized by ITIN for both branches. The proposed design is able to switch between these two branches by the feedback network according to its output voltage level. The rectifier has been simulated, fabricated, and tested. The measured power conversion efficiency (PCE) exceeds 50% over the input power range from 5 to 29 dBm, with a total dynamic range of 24 dB. The input range when PCE exceeds 60% is from 10 dBm to 28 dBm. The maximum efficiency is 75.2% at 26 dBm input power.

Keywords: wireless power transfer (WPT); self-biased circuit; input power range; power conversion efficiency (PCE); RF-rectifiers

1. Introduction

The microwave power transfer (MPT) system is designed to transmit and collect energy wirelessly through free space and converts received RF signal to DC currents for power supply [1–3]. MPT eliminates the need for cables and waveguides. Thus, it serves as an additional source of energy [4] and could be applied to scenarios that are beyond the reach of conventional methods. It has drawn increasing attention due to its potential contribution to green energy applications [5–12] and has been applied to applications such as space solar power satellites (SSPS) and power supply for high-altitude aircraft and drones. In recent years, the number of wireless charging devices is expected to increase after the concept of the Internet of Things (IoT) [13,14], especially when MPT is integrated with Mobile Edge Cloud (MEC) [15].

Despite its unique advantages, a significant advance in transmission efficiency is still required when it comes to practical applications [8]. One of the paramount problems at the receiver end is to improve rectification efficiency. The RF-rectifier comprises a rectifying diode, a DC-pass filter, and a load match by an impedance matching network [16,17]. In previous literature, rectifiers of different topologies, such as band-stop structure [18], bridge diode [19], Branch-line coupler [20,21], and rectifiers adopting GaN Schottky barrier diode [22,23], GaAs Schottky diodes [24], and reconfigurable hybrid structure [25] have been proposed to achieve high efficiency.

Due to the nonlinear characteristics of the Schottky diode, however, rectifiers could only achieve ideal efficiency at a given input power range. Otherwise, conversion efficiency will deteriorate rapidly [26]. In practical applications, the distance and incident angle from the RF source to the rectennas or harvester is very diverse, which greatly affects received RF power. The input power of the rectifier is not likely to always stay in the designed range, which will lead to very low efficiency in some circumstances. Thus, it is desirable to maintain high conversion efficiency over a wide input power range.

For rectifiers with a wide power input range, previous research has introduced techniques such as transmission-line-based resistance compression networks [27,28], branch-line couplers [21,29], and cooperative structure [30,31], which has presented a dual-channel



Citation: Lai, S.; Zhang, Z.; Liu, Z.; Wang, G.; Zhou, Y.; Zhu, H.; Yang, Y. A Novel Self-Adaptive Rectifier with High Efficiency and Wide Input Power Range. *Electronics* **2023**, *12*, 712. <https://doi.org/10.3390/electronics12030712>

Academic Editor: Fabio Corti

Received: 5 January 2023

Revised: 25 January 2023

Accepted: 30 January 2023

Published: 31 January 2023



Copyright: © 2023 by the authors. Licensee MDPI, Basel, Switzerland. This article is an open access article distributed under the terms and conditions of the Creative Commons Attribution (CC BY) license (<https://creativecommons.org/licenses/by/4.0/>).

rectifier with a Wilkinson power divider. The power dynamic range for efficiency of 50% is expanded by 2 dBm compared with a single HSMS2860 rectifier branch. In [32], He proposed a compact rectifier with a wide input power range, leveraging the nonlinear characteristics of the diodes. It achieves an RF-DC conversion efficiency exceeding 50% over an input range of 23.3 dB (from 6.5 to 29.8 dBm), with a maximum efficiency of 74.5% at 27 dBm input power. In [33], Lu et al. introduced a self-tuning matching structure to extend its input power range. The proposed rectenna reaches more than 50% conversion efficiency over a broadened input power range from -6 – 21 dB with a peak efficiency of 78.2%. [34] presents an auto-adaptive impedance matching for rectifiers. The strategy improves the efficiency of the system by up to 20%. [35] presents a reconfigurable harvesting device that consists of a passive RF detector, a three-level logic comparator, and three antenna switches. However, the detection and calculation units will increase the cost and size of the rectifier, and it will take an extra power supply to support the system. A novel dual-band rectifier with an extended power range and an optimal incident RF power strategy in settings where the available RF energy fluctuates considerably has been presented in [36]. A peak conversion efficiency of 60% was maintained from 5 to 15 dBm.

In this paper, we propose a novel rectifier with high efficiency and a wide input power range. The proposed rectifier consists of two sub-rectifier branches, an ITIN and a feedback network. The two sub-rectifier branches are self-biased and controlled by the feedback network according to the output voltage level. The ITIN network is able to improve the matching performance at high and low power levels, respectively. The rectifier has been fabricated and tested, achieving high efficiency over a wide input power range. Compared with [30,35], the load impedances at different power levels are constant. It does not involve logic comparators and MCUs like [35] does. Due to good matching performance, the input range for efficiency at higher efficiency is wider than that in [32]. The proposed rectifier has advantages in terms of high efficiency, wide input power range, reconfigurability, and easiness of integration.

2. Circuit Realization

The 2.45 GHz self-adaptive rectifier is shown in Figure 1. The overall design mainly consists of two sub-rectifiers branches operating at low and high-power levels, controlled by the feedback network. Between the two branches, there is a network for impedance matching and isolation of the two branches. A capacitor was used at the input port to block the reverse current. A DC-pass filter was deployed between the sub-rectifier branches and the load to suppress harmonics generated by the diode during rectification.

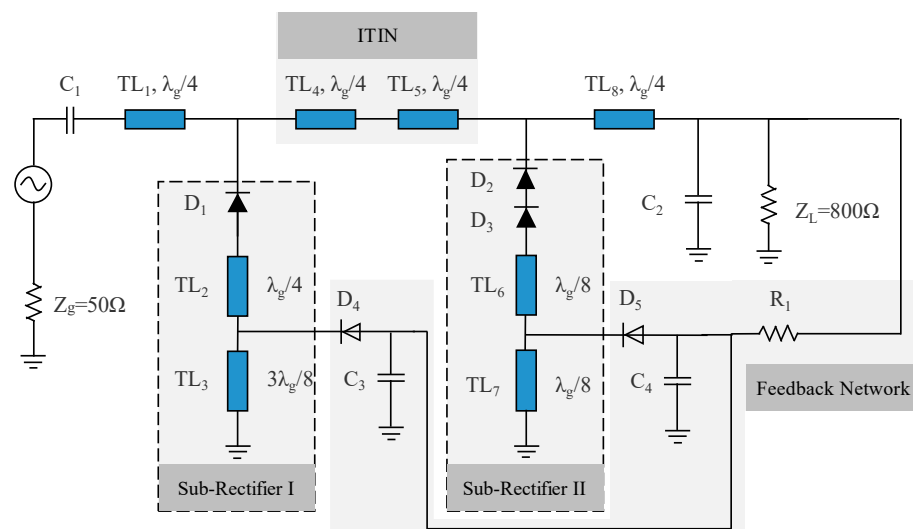


Figure 1. Schematic of the proposed rectifier.

2.1. Design of Rectifier Branches and Feedback Network

In [18], Liu proposed a rectifier in series with a short-ended eighth-wavelength microstrip transmission line which works as a band-stop structure, as given in Figure 2. The proposed structure aims to compensate the diode capacitive impedance and turns to an open circuit to block the second harmonic for power recycling. In order to realize high efficiency over a wide input power range, two sub-rectifier branches I and II are designed based on [18] for low-power and high-power rectification, respectively, which are presented in Figure 3a,b. The adopted Schottky diodes $D_1, D_2,$ and D_3 are HSMS282 with low junction capacitance ($C_{j0} = 0.7$ pF), low series resistance ($R_s = 6 \Omega$), and low forward voltage ($V_F = 0.25$ V).

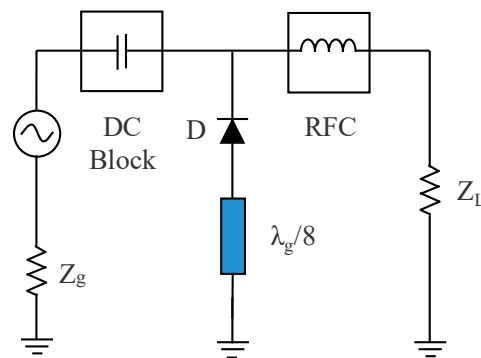


Figure 2. Rectifier with a band-stop structure.

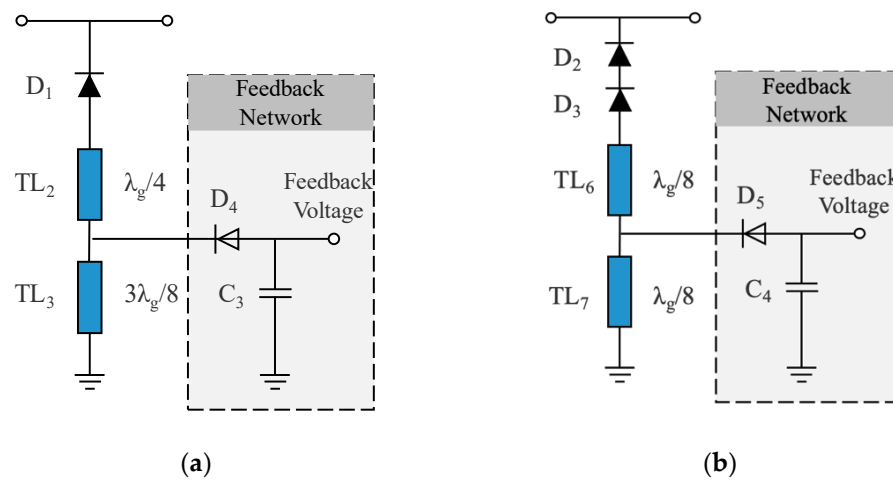


Figure 3. Design of the sub-rectifiers: (a) Sub-rectifier I; (b) Sub-rectifier II.

The low-power sub-rectifier I is given in Figure 3a. It consists of an HSMS282 diode, a series quarter-length transmission line, and a series short-ended three-eighths-length transmission line. It is designed to implement rectification with about 16-dBm input power at ISM frequency 2.45 GHz. The high-power sub-rectifier is given in Figure 3b. It consists of two HSMS282 diodes, a series eighth-length transmission line, and a series short-ended eighth-length transmission line. It is designed to implement rectification with about 26-dBm input power at ISM frequency 2.45 GHz.

The input impedance Z_{in} of the eighth-wavelength short-ended transmission line is

$$Z_{in} = jZ_{SE} \tan \beta l = jZ_{SE} \tan \left(\frac{2\pi}{\lambda} \cdot \frac{\lambda}{8} \right) = jZ_{SE} \tag{1}$$

where Z_{SE} is the characteristic impedance of the eighth-wavelength short-ended transmission line.

In order to compensate for the diode capacitive impedance, Z_{SE} should follow the below relation,

$$Z_{SE} = -Im\{Z_D\} \tag{2}$$

where Z_D is the diode impedance.

Therefore, the characteristic impedances of the microstrip lines $TL_2, TL_3, TL_6,$ and TL_7 are obtained from Equation (2) and their respective line widths are determined.

The feedback network, as shown in Figure 1, consists of a bias resistor R_1 , two capacitors C_3 and C_4 , and two p-i-n diodes BAR64-02V from Infineon. The two p-i-n diodes are driven by output DC voltage. Bias resistor R_1 is deployed between the load and the diodes to control the applied voltage to the p-i-n diodes. Since the resistance is large, the feedback network only occupies a very small proportion of output power, which could be neglected. Capacitor C_1 and C_2 not only block DC current but also short-circuit RF signal when the diode is in forward bias. DC current passes the diodes and is short-circuited by the lines connected to the ground (TL_3 and TL_7), which eliminates the need for extra blocking capacitors.

For the low-power branch (Sub-rectifier I), without feedback voltage, the diode is in reverse bias. The feedback network is disconnected from Sub-rectifier I. Thus, the length of the transmission line connected to diode D_1 is $5\lambda/8$, which is equivalent to $\lambda/8$ according to transmission line theory. The circuit is equivalent to that in Figure 2 and rectification is turned on. With feedback voltage, the input impedance of the feedback network is close to zero. Thus, TL_3 is short-circuited. Sub-rectifier I is equivalent to a diode in series with a short-ended $\lambda/4$ TL_2 . The input impedance of TL_2 under such circumstances is a very large value. RF signal is blocked at the designed frequency. Thus, rectification is turned off.

For the high-power branch (Sub-rectifier II), without feedback voltage, the diode is in reverse bias. The feedback network is disconnected from Sub-rectifier II. Thus, the length of the transmission line connected to diodes D_2 and D_3 is $\lambda/4$. The input impedance of TL_6 and TL_7 in series is a very large value. RF signal is blocked at the designed frequency. Thus, rectification is turned off. With feedback voltage, the input impedance of the feedback network is close to zero. Thus, TL_7 is short-circuited and the transmission line connected to diodes D_2 and D_3 is $\lambda/8$ in length. The circuit is equivalent to that in Figure 2 and rectification is turned on.

By applying output voltage to the feedback network, we can either turn on sub-rectifier I and turn off sub-rectifier II when the input power level is low or turn off sub-rectifier I and turn on sub-rectifier II when the input power level is high, thereby enabling the automatic switch from the two sub-rectifier branches according to input power level. Additional bias network is eliminated, and the bias power is supplied by the rectifier circuit itself.

2.2. Design of the Impedance Transform and Isolation Network (ITIN)

The impedance of the Schottky diodes could be obtained by the following equation [37]

$$Z_D = \frac{\pi R_S}{\cos\theta_{on} \left(\frac{\theta_{on}}{\cos\theta_{on}} - \sin\theta_{on} \right) + j\omega R_S C_j \left(\frac{\pi - \theta_{on}}{\cos\theta_{on}} + \sin\theta_{on} \right)} \tag{3}$$

where θ_{on} is the turn-on angle of the diode, and the junction capacitance of the diode is

$$C_j = C_{j0} \sqrt{\frac{V_{bi}}{V_0 + V_{bi}}} \tag{4}$$

where V_0 is the output DC voltage and V_{bi} is the diode's built-in voltage in the forward bias region (for HSMS282, $V_{bi} = 0.25$ V). From the above equations, we can obtain the impedances of the two branches Z_{D1} and Z_{D2} , respectively.

The proposed ITIN consists of two quarter-wavelength transmission lines TL_4 and TL_5 . The characteristic impedances of the two lines are $Z_{TL4} = Re\{Z_{D1}\}$ and $Z_{TL5} = (Re\{Z_{D1}\} \cdot Re\{Z_{D2}\})^{1/2}$.

It is designed to isolate the two branches at the low-power level and transform the input impedance of sub-rectifier II to the impedance of sub-rectifier I at high-power level.

The equivalent circuits at low and high-power levels are given in Figure 4a,b.

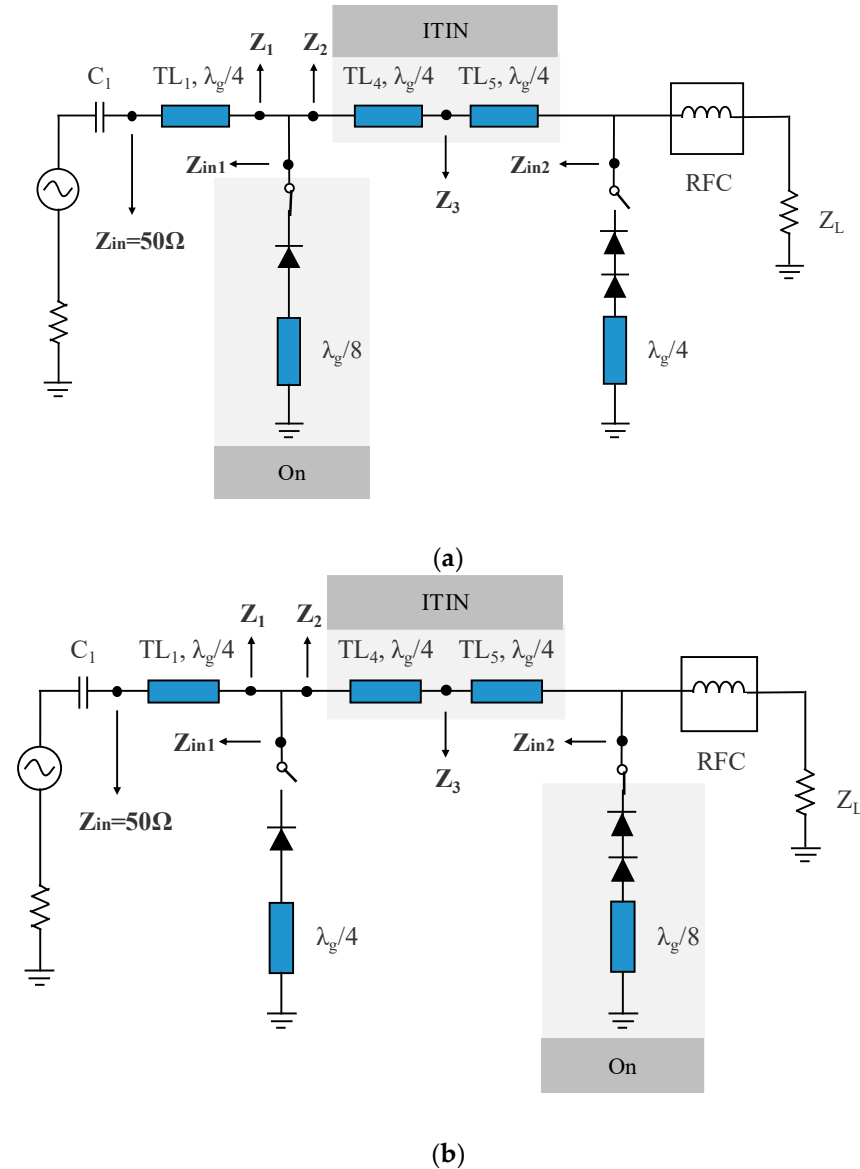


Figure 4. Equivalent circuit of the proposed rectifier: (a) Low-power level; (b) High-power level.

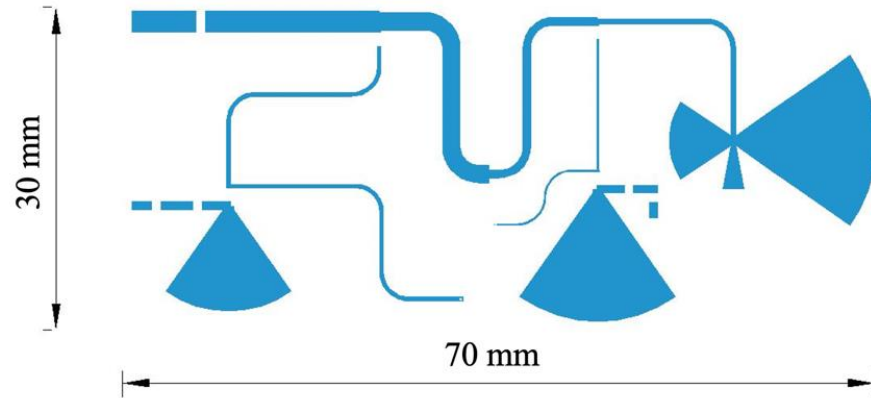
At the low-power level, as illustrated in Figure 4a, sub-rectifier I is turned on and II is turned off. Z_{in2} tends to be ∞ . The electrical length of TL_4 and TL_5 combined is $\lambda/2$. Thus, $Z_2 = Z_{in2} = \infty$ and the two branches are isolated. Without TL_4 , sub-rectifier I will be short-ended. Meanwhile, $Z_{in1} = \text{Re}\{Z_{D1}\}$. $Z_1 = \text{Re}\{Z_{D1}\}$ and is transformed to input impedance $Z_{in} = 50 \Omega$ by TL_1 .

At the high-power level, as illustrated in Figure 4b, sub-rectifier II is turned on and I is turned off. $Z_{in2} = \text{Re}\{Z_{D2}\}$. It is transformed to $Z_3 = \text{Re}\{Z_{D1}\}$ after TL_5 . $Z_2 = Z_3 = \text{Re}\{Z_{D1}\}$. Meanwhile, Z_{in1} tends to be ∞ . $Z_1 = \text{Re}\{Z_{D1}\}$ and is transformed to input impedance $Z_{in} = 50 \Omega$ by TL_1 .

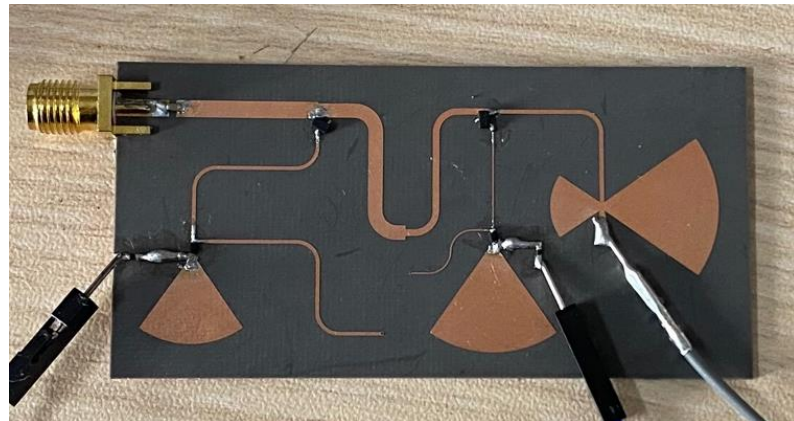
From the above analysis, the proposed design is able to isolate the two branches at the low-power level and transform the input impedance of sub-rectifier II to the impedance of sub-rectifier I at the high-power level. $Z_1 = \text{Re}\{Z_{D1}\}$ at both high and low power levels and is transformed to input impedance $Z_{in} = 50 \Omega$ by TL_1 .

3. Simulation and Experiment Results

The proposed rectifier has been optimized, fabricated, and tested for validation. The substrate is Rogers 5880 ($\epsilon_r = 2.2$ and $\tan\delta = 0.0009$), with a thickness of 0.787 mm. The circuit layout is given in Figure 5a. The simulation is executed by Advanced Design System (ADS). Input power is provided by a signal generator. The output voltage is measured by a voltage meter. Output DC load is a standard resistor box.



(a)



(b)

Figure 5. Proposed rectifier: (a) Layout; (b) Fabricated circuit.

The microwave-to-DC conversion efficiency η of the rectifier is defined as

$$\eta = \frac{P_{DC}}{P_{in}} \times 100\% = \frac{V_0^2}{P_{in} \cdot Z_L} \times 100\% \quad (5)$$

where P_{DC} is the DC output power at load Z_L , P_{in} is the input power of the microwave source, V_0 is the output DC voltage, and Z_L is the DC load.

The simulation and measurement results are shown in Figure 6, which are in accordance with simulation. The conversion efficiency exceeds 50% over the input power range from 5 to 29 dBm, with a total dynamic range of 24 dB. The conversion efficiency of over 60% is from 10 dBm to 28 dBm. Maximum efficiency is 75.2% at 26 dBm. The proposed design achieves a wide input power range and high efficiency at a relatively high-power input range. The comparison of the proposed design with some recently published wide-input-power-range rectifiers is displayed in Table 1.

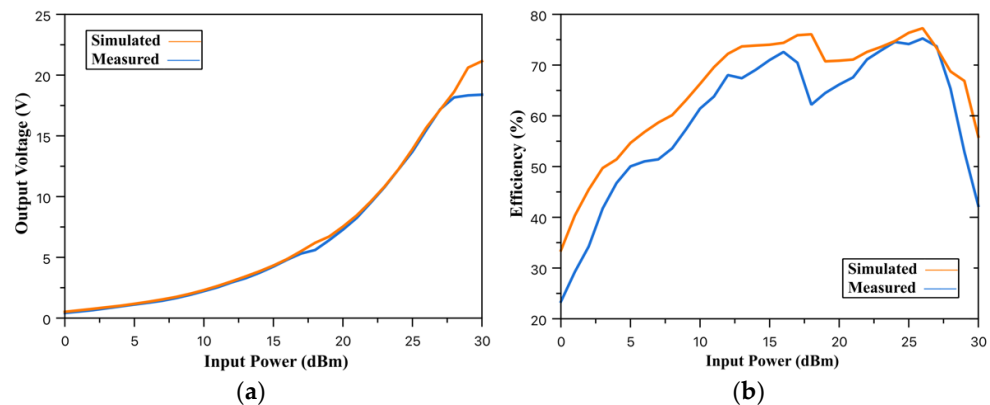


Figure 6. Simulation and experiment results: (a) Output voltage; (b) Output efficiency.

Table 1. Comparison of rectifiers with wide input power range.

Ref.	Freq. (GHz)	Pin (dBm) Range for Eff. > 50%	Max. Eff. (%)	Methods	Extra Power Supply	Constant Load Impedance
[31]	2.45	8~27	75.5	Wilkinson power divider	No	No
[29]	2.45	2.9~20.2	80.8	Coupler	No	No
[30]	2.4	-3.5~26	72.8	Cooperative	No	No
[32]	2.45	6.5~29.8	74.5	Non-linear power division	No	Yes
[33]	2.45	-6~21	78.2	Self-biased network	No	Yes
[34]	2.45	-3~22	78	SPDT	Yes	No
This work	2.45	5~29	75.2%	Self-adaptive Branches	No	Yes

Compared with existing works in [29,30,33,34], the proposed design achieves a higher overall input power level. Note that our design is not aimed at achieving the best conversion efficiency or input power range. We have taken whether load impedance is constant, whether the circuit needs extra power supply, and impedance matching performance into consideration. For example, the designs in [30,35] achieve high efficiencies and wide input ranges. However, their load impedances at different power levels are not constant. In practical applications, the rectenna arrays are usually connected to the same load. Under such circumstances, the designs in [30,35] may not be applicable. Besides, the design in [35] consists of logic comparators and MCUs, which require an extra power supply. In [32], a non-linear power division strategy is adopted. Input power is divided according to the impedance variation of the two branches. It achieves a wide input range at a compact size. However, the circuit is mismatched. By contrast, in our design, due to the ITIN network, the circuit is matched when input power is 16 dBm and 26 dBm, respectively, achieving a better input range for efficiency >60% and efficiency >70%. Besides, the output impedance is constant, and no extra power supply is required.

The proposed design is not only suitable for traditional high-power MPT applications, such as SSPS and power supply for high-altitude aircraft and drones, but could also be applied to Wireless Power Mobile Edge Cloud (WPMEC). The WPMEC system adopts a time division multiplexing strategy. During the energy transfer period, the battery is charged. During the communication period, the battery supplies the communication circuit [15]. Higher power input is able to support devices with higher computational power. Meanwhile, it makes fast charging possible, which leaves a longer time period for communication. This investigation provides a good reference for future energy harvesting system design.

4. Conclusions

We have proposed a novel self-adaptive rectifier with high efficiency and a wide input power range which consists of two sub-rectifier branches for low and high power, an ITIN, and a feedback network. The rectifier is able to switch between these two branches according to output voltage, thus expanding its input power range. The ITIN network can

improve the matching performance at high and low power levels, respectively. The circuit has been simulated, fabricated, and tested. The conversion efficiency exceeds 50% over the input power range from 5 to 29 dBm, with a total dynamic range of 24 dB. The conversion efficiency of over 60% is from 10 dBm to 28 dBm. The maximum efficiency is 75.2% at 26 dBm. The proposed design demonstrates great potential in future WPT applications.

Author Contributions: Conceptualization, S.L. and Y.Y.; Formal analysis, S.L.; Methodology, S.L.; Resources, H.Z. and Y.Y.; Supervision, H.Z. and Y.Y.; Validation, S.L., Z.Z., Z.L. and G.W.; Writing—original draft, S.L.; Writing—review & editing, S.L., Z.Z., Z.L., G.W., Y.Z., H.Z. and Y.Y. All authors have read and agreed to the published version of the manuscript.

Funding: This research was funded by Sichuan Science and Technology Program (No. 2021YFG0265).

Data Availability Statement: The data presented in this study are available on request from the corresponding author.

Conflicts of Interest: The authors declare no conflict of interest.

References

1. Erkmen, F.; Almoneef, T.S.; Ramahi, O.M. Electromagnetic Energy Harvesting Using Full-Wave Rectification. *IEEE Trans. Microw. Theory Tech.* **2017**, *65*, 1843–1851. [[CrossRef](#)]
2. Ashoor, A.Z.; Almoneef, T.S.; Ramahi, O.M. A Planar Dipole Array Surface for Electromagnetic Energy Harvesting and Wireless Power Transfer. *IEEE Trans. Microw. Theory Tech.* **2018**, *66*, 1553–1560. [[CrossRef](#)]
3. Bolos, F.; Blanco, J.; Collado, A.; Georgiadis, A. RF Energy Harvesting from Multi-Tone and Digitally Modulated Signals. *IEEE Trans. Microw. Theory Tech.* **2016**, *64*, 1918–1927. [[CrossRef](#)]
4. Muhammad, S.; Tiang, J.J.; Wong, S.K.; Rambe, A.H.; Adam, I.; Smida, A.; Waly, M.I.; Iqbal, A.; Abubakar, A.S.; Mohd Yasin, M.N. Harvesting Systems for RF Energy: Trends, Challenges, Techniques, and Tradeoffs. *Electronics* **2022**, *11*, 959. [[CrossRef](#)]
5. Brown, W. Adapting Microwave Techniques to Help Solve Future Energy Problems. *IEEE Trans. Microw. Theory Tech.* **1973**, *21*, 753–763. [[CrossRef](#)]
6. Brown, W.; Eves, E. Beamed microwave power transmission and its application to space. *IEEE Trans. Microw. Theory Tech.* **1992**, *40*, 1239–1250. [[CrossRef](#)]
7. Glaser, P. An overview of the solar power satellite option. *IEEE Trans. Microw. Theory Tech.* **1992**, *40*, 1230–1238. [[CrossRef](#)]
8. McSpadden, J.O.; Mankins, J.C. Space solar power programs and microwave wireless power transmission technology. *IEEE Microw. Mag.* **2002**, *3*, 46–57. [[CrossRef](#)]
9. Matsumoto, H. Research on solar power satellites and microwave power transmission in Japan. *IEEE Microw. Mag.* **2002**, *3*, 36–45. [[CrossRef](#)]
10. Sasaki, S.; Tanaka, K. Wireless power transmission technologies for solar power satellite. In Proceedings of the 2011 IEEE MTT-S International Microwave Workshop Series on Innovative Wireless Power Transmission: Technologies, Systems, and Applications, Kyoto, Japan, 12–13 May 2011; pp. 3–6.
11. Strassner, B.; Chang, K. Microwave Power Transmission: Historical Milestones and System Components. *IEEE Proc.* **2013**, *101*, 1379–1396. [[CrossRef](#)]
12. Sasaki, S.; Tanaka, K.; Maki, K.I. Microwave Power Transmission Technologies for Solar Power Satellites. *IEEE Proc.* **2013**, *101*, 1438–1447. [[CrossRef](#)]
13. Hashimoto, T.; Tanzawa, T. Design Space Exploration of Antenna Impedance and On-Chip Rectifier for Microwave Wireless Power Transfer. *Electronics* **2022**, *11*, 3218. [[CrossRef](#)]
14. Nusrat, T.; Roy, S.; Lotfi-Neyestanak, A.A.; Noghianian, S. Far-Field Wireless Power Transfer for the Internet of Things. *Electronics* **2023**, *12*, 207. [[CrossRef](#)]
15. Mahmood, A.; Ahmed, A.; Naeem, M.; Hong, Y. Partial Offloading in Energy Harvested Mobile Edge Computing: A Direct Search Approach. *IEEE Access* **2020**, *8*, 36757–36763. [[CrossRef](#)]
16. Singh, J.; Kaur, R.; Singh, D. Energy harvesting in wireless sensor networks: A taxonomic survey. *Int. J. Energy Res.* **2021**, *45*, 118–140. [[CrossRef](#)]
17. Valenta, C.R.; Durgin, G.D. Harvesting wireless power: Survey of energy-harvester conversion efficiency in far-field, wireless power transfer systems. *IEEE Microw. Mag.* **2014**, *15*, 108–120.
18. Liu, C.; Tan, F.; Zhang, H.; He, Q. A Novel Single-Diode Microwave Rectifier with a Series Band-Stop Structure. *IEEE Trans. Microw. Theory Tech.* **2017**, *65*, 600–606. [[CrossRef](#)]
19. Sakai, N.; Noguchi, K.; Itoh, K. A 5.8-GHz Band Highly Efficient 1-W Rectenna with Short-Stub-Connected High-Impedance Dipole Antenna. *IEEE Trans. Microw. Theory Tech.* **2021**, *69*, 3558–3566. [[CrossRef](#)]
20. Wang, S.C.; Li, M.J.; Tong, M.S. A Miniaturized High-Efficiency Rectifier with Extended Input Power Range for Wireless Power Harvesting. *IEEE Microw. Wirel. Compon. Lett.* **2020**, *30*, 617–620. [[CrossRef](#)]

21. Xiao, Y.Y.; Du, Z.X.; Zhang, X.Y. High-Efficiency Rectifier with Wide Input Power Range Based on Power Recycling. *IEEE Trans. Circuits Syst. II Exp. Briefs* **2018**, *65*, 744–748. [[CrossRef](#)]
22. Dang, K.; Zhang, J.; Zhou, H.; Huang, S.; Zhang, T.; Bian, Z.; Zhang, Y.; Wang, X.; Zhao, S.; Wei, K.; et al. A 5.8-GHz High-Power and High-Efficiency Rectifier Circuit with Lateral GaN Schottky Diode for Wireless Power Transfer. *IEEE Trans. Power Electron.* **2020**, *35*, 2247–2252. [[CrossRef](#)]
23. Li, Y.; Pu, T.F.; Li, X.B.; Zhong, Y.R.; Yang, L.A.; Fujiwara, S.; Kitahata, H.; Ao, J.P. GaN Schottky Barrier Diode-Based Wideband and Medium-Power Microwave Rectifier for Wireless Power Transmission. *IEEE Trans. Electron. Devices* **2020**, *67*, 4123–4129. [[CrossRef](#)]
24. Wang, C.; Yang, B.; Shinohara, N. Study and Design of a 2.45-GHz Rectifier Achieving 91% Efficiency at 5-W Input Power. *IEEE Microw. Wirel. Compon. Lett.* **2021**, *31*, 76–79. [[CrossRef](#)]
25. Lian, W.X.; Yong, J.K.; Chong, G.; Churchill, K.K.P.; Ramiah, H.; Chen, Y.; Mak, P.-I.; Martins, R.P. A Reconfigurable Hybrid RF Front-End Rectifier for Dynamic PCE Enhancement of Ambient RF Energy Harvesting Systems. *Electronics* **2023**, *12*, 175. [[CrossRef](#)]
26. Takhedmit, H.; Merabet, B.; Cirio, L.; Allard, B.; Costa, F.; Vollaïre, C.; Picon, O. A 2.45-GHz dual-diode RF-to-DC rectifier for rectenna applications. In Proceedings of the 40th European Microwave Conference, Paris, France, 28–30 September 2010; pp. 37–40.
27. Liu, J.; Zhang, X.Y.; Xue, Q. Dual-Band Transmission-Line Resistance Compression Network and Its Application to Rectifiers. *IEEE Trans. Circuits Syst. I Reg. Papers* **2019**, *66*, 119–132. [[CrossRef](#)]
28. Barton, T.W.; Gordonson, J.; Perreault, D.J. Transmission line resistance compression networks for microwave rectifiers. In Proceedings of the 2014 IEEE MTT-S International Microwave Symposium (IMS2014), Tampa, FL, USA, 1–6 June 2014; pp. 1–4.
29. Zhang, X.Y.; Du, Z.X.; Xue, Q. High-Efficiency Broadband Rectifier with Wide Ranges of Input Power and Output Load Based on Branch-Line Coupler. *IEEE Trans. Circuits Syst. I Reg. Papers* **2017**, *64*, 731–739. [[CrossRef](#)]
30. Zheng, S.Y.; Wang, S.H.; Leung, K.W.; Chan, W.S.; Xia, M.H. A High-Efficiency Rectifier with Ultra-Wide Input Power Range Based on Cooperative Structure. *IEEE Trans. Microw. Theory Tech.* **2019**, *67*, 4524–4533. [[CrossRef](#)]
31. Peng, C.; Ye, Z.; Wu, J.; Chen, C.; Wang, Z. Design of a Wide-Dynamic RF-DC Rectifier Circuit Based on an Unequal Wilkinson Power Divider. *Electronics* **2021**, *10*, 2815. [[CrossRef](#)]
32. He, Z.; Lan, J.; Liu, C. Compact Rectifiers with Ultra-wide Input Power Range Based on Nonlinear Impedance Characteristics of Schottky Diodes. *IEEE Trans. Power Electron.* **2021**, *36*, 7407–7411. [[CrossRef](#)]
33. Lu, P.; Song, C.; Cheng, F.; Zhang, B.; Huang, K. A Self-Biased Adaptive Reconfigurable Rectenna for Microwave Power Transmission. *IEEE Trans. Ind. Electron.* **2020**, *35*, 7749–7754. [[CrossRef](#)]
34. Mirzavand, F.; Nayyeri, V.; Soleimani, M.; Mirzavand, R. Efficiency improvement of WPT system using inexpensive auto-adaptive impedance matching. *Electron. Lett.* **2016**, *52*, 2055–2057. [[CrossRef](#)]
35. Marian, V.; Allard, B.; Vollaïre, C.; Verdier, J. Strategy for Microwave Energy Harvesting from Ambient Field or a Feeding Source. *IEEE Trans. Power Electron.* **2012**, *27*, 4481–4491. [[CrossRef](#)]
36. Liu, Z.; Zhong, Z.; Guo, Y.X. Enhanced Dual-Band Ambient RF Energy Harvesting with Ultra-Wide Power Range. *IEEE Microw. Wirel. Compon. Lett.* **2015**, *25*, 630–632. [[CrossRef](#)]
37. McSpadden, J.O.; Fan, L.; Chang, K. Design and experiments of a high-conversion-efficiency 5.8-GHz rectenna. *IEEE Trans. Microw. Theory Tech.* **1998**, *46*, 2053–2060. [[CrossRef](#)]

Disclaimer/Publisher’s Note: The statements, opinions and data contained in all publications are solely those of the individual author(s) and contributor(s) and not of MDPI and/or the editor(s). MDPI and/or the editor(s) disclaim responsibility for any injury to people or property resulting from any ideas, methods, instructions or products referred to in the content.